applied sciences

MDPI

Article

Advancements in Roundness Measurement Parts for Industrial Automation Using Internet of Things Architecture-Based Computer Vision and Image Processing Techniques

Yazid Saif [1], Anika Zafiah M. Rus [1,*], Yusri Yusof [1], Maznah Lliyas Ahmed [2,*], Sami Al-Alimi [1], Djamal Hissein Didane [1], Anbia Adam [3], Yeong Hyeon Gu [4,*], Mohammed A. Al-masni [4] and Hakim Qaid Abdullah Abdulrab [5]

1 Faculty of Mechanical and Manufacturing Engineering, Universiti Tun Hussein Onn Malaysia, Parit Raja 86400, Johor, Malaysia; yazeedalkosa@gmail.com (Y.S.); yusri@uthm.edu.my (Y.Y.); samialalimi@gmail.com (S.A.-A.); djamal@uthm.edu.my (D.H.D.)
2 Politeknik Sultan Azlan Shah, Behrang Stesion, Behrang 35950, Perak, Malaysia
3 Faculty of Mechanical and Manufacturing Engineering Technology, Universiti Teknikal Malaysia Meleka (UTeM), Durian Tunggal 76100, Melaka, Malaysia; anbia@utem.edu.my
4 Department of Artificial Intelligence, College of Software and Convergence Technology, Sejong University, Seoul 05006, Republic of Korea; m.almasani@sejong.ac.kr
5 Department of Electrical and Electronics Engineering, University Teknologi PETRONAS, Seri Iskandar 32610, Perak, Malaysia; hakim_19001004@utp.edu.my
* Correspondence: zafiah@uthm.edu.my (A.Z.M.R.); maznah.iliyas@psas.edu.my (M.L.A.); yhgu@sejong.ac.kr (Y.H.G.)

Abstract: In the era of Industry 4.0, the digital capture of products has become a critical aspect, which prompts the need for reliable inspection methods. In the current technological landscape, the Internet of Things (IoT) holds significant value, especially for industrial devices that require seamless communication with local and cloud computing servers. This research focuses on the advancements made in roundness measurement techniques for industrial automation by leveraging an IoT architecture, computer vision, and image processing. The interconnectedness enables the efficient collection of feedback information, meeting the demands of closed-loop manufacturing. The accuracy and performance of assemblies heavily rely on the roundness of specific workpiece components. In order to address this problem, automated inspection methods are needed. A new method of computer vision for measuring and inspecting roundness is proposed in this paper. This method uses a non-contact method that takes into account all points on the contours of measured objects, making it more accurate and practical than conventional methods. The system developed by AMMC Laboratory captures Delrin work images and analyzes them using a specially designed 3SMVI system based on Open CV with Python script language. The system can measure and inspect several rounded components in the same part, including external frames and internal holes. It is calibrated to accommodate various units of measurement and has been tested using sample holes within the surface feature of the workpiece. According to the results of both techniques, there is a noticeable difference ranging from 2.9 µm to 11.6 µm. However, the accuracy of the measurements can be enhanced by utilizing a high-resolution camera with proper lighting. The results were compared to those obtained using a computer measurement machine (CMM), with a maximum difference of 8.7%.

Keywords: computer vision; image processing; CMM; 3SMVI; inspection; IoT; roundness

Citation: Saif, Y.; Rus, A.Z.M.; Yusof, Y.; Ahmed, M.L.; Al-Alimi, S.; Didane, D.H.; Adam, A.; Gu, Y.H.; Al-masni, M.A.; Abdulrab, H.Q.A. Advancements in Roundness Measurement Parts for Industrial Automation Using Internet of Things Architecture-Based Computer Vision and Image Processing Techniques. *Appl. Sci.* **2023**, *13*, 11419. https://doi.org/10.3390/app132011419

Academic Editors: Tibor Krenicky, Juraj Ruzbarsky and Maros Korenko

Received: 18 July 2023
Revised: 15 October 2023
Accepted: 16 October 2023
Published: 18 October 2023

1. Introduction

In the present fast-changing industrial world driven by globalization, product customization, and automation, the manufacturing industry plays a crucial role. With advanced technologies and techniques that enable rapid and efficient changes in products,

processes, and supply chains, the manufacturing industry is at the forefront of Industry 4.0. In the realm of advanced manufacturing systems, manufacturing metrology holds significant importance as it pertains to the measurement and inspection of nearly all machined objects. The advent of Industry 4.0 brings forth novel methodologies for the development of next-generation manufacturing metrology systems that possess characteristics such as intelligence, autonomy, flexibility, interoperability, high productivity, and self-adaptability [1]. Furthermore, a significant shift is generally known as the fourth industrial revolution (IR 4.0) [2]. Emerging technologies such as machine learning, artificial intelligence, big data, 3D printing, and robotics are constantly evolving within the realm of IoT (Internet of Things). The rapid progress of these technologies brings about substantial transformations, as IoT enables devices to perceive and interact with the surrounding environment, imbuing them with a sense of vitality. This industrial decentralization has paved the way for the efficient and remote control and monitoring of industrial operations. Given that IoT represents the future of computing, it requires the synergistic support of pioneering technologies to facilitate its growth and development [3,4]. IoT provides a wide variety of digital and physical resources for I 4.0. Thus, the established network allows for decentralized decision-making and reacting to cyber–physical systems (CPS) in real time [5]. In addition, a computer vision system contains smart Internet of Things (IoT) cameras looking directly at the production line that capture images, which are then algorithmically compared to a predefined image to detect defective objects [6]. The IoT and digital manufacturing industry significantly accelerate product development, producing products with complexity and precision that previously could not be created by cycles and manufacturers [7].

Circular features are among the fundamental geometric elements of mechanical parts. The performance and lifespan of mechanical products depend on how accurately and efficiently circularity errors can be evaluated [8]. To determine the degree of roundness of rounded parts, the entire profile should be measured in accordance with the geometric roundness tolerance standard [9]. The mission is to use machine vision to inspect an automotive camshaft for roundness errors in real time. Further measurement studies are required to improve accuracy and efficiency in roundness error measurement in order to achieve successful roundness evaluation of the part using image processing procedures and mathematical models [10–13]. Coordinate metrology is an essential inspection tool for ensuring quality in machined workpieces. It can analyze the impact of parameters on milled pocket diameter and roundness accuracy using CNC and CMM specimens, address measurement deviations, and estimate uncertainty using statistical repeatability analysis [14]. The measurement of circular sector elements requires appropriate control, which is driven by the increasing demand for complete control of specific geometrical features [15–17]. Conventional instruments have limitations in their sampling points, making it difficult or impossible to meet current roundness measurement standards. Furthermore, using such instruments to measure the entire profile of rounded parts increases the process's complexity and duration. Coordinate measuring machines (CMMs) are becoming more common in automated inspections of manufactured components, both online and offline, to meet geometric roundness tolerance standards. In the measurement of roundness errors, coordinate measuring machines (CMMs) rely on capturing data from various sampling points along the profile of curved parts. However, the use of CMMs for this purpose can be both resource-intensive and time-consuming, particularly when a large number of points need to be measured [18–20].

The availability of inexpensive digital computers has made it possible to incorporate machine vision systems into automated manufacturing systems without a large financial burden. The progress in machine vision, image processing, computational intelligence, and similar areas has significantly improved the potential of visual inspection methods [21–23]. A stereo vision and image analysis system for automating workpiece referencing in three-axis machining centers is presented. The system captures images with two cameras, which are then processed in custom software to return workpiece

coordinates to machining workers [24]. A cloud-based system uses stereo vision and image analysis to automate workpiece referencing in machining companies. The system processes images from two cameras in the spindle in custom software and returns the Workpiece Coordinate System (WCS) position to the CNC machine controller. Experiment results validate the application in actual machining processes [25]. In comparison to coordinate measuring machines (CMMs), a machine vision system equipped with a standard 512 × 512 image processor can gather a large number of boundary points in a short period. Furthermore, machine vision can conduct non-contact inspections of products, whereas most instruments used to measure roundness require physical contact. As a consequence, there has been significant interest in developing machine vision systems for inspection in the industrial sector [2,26–31]. A machine vision-based inspection system has been addressed for real-time geometric inspection of A-grade nuts to ensure their quality. The algorithm was optimized for accuracy and usability, resulting in faster and more appropriate nut detection, making it suitable for all testing processes [32]. Machine vision systems provide benefits such as faster measurement times, improved accuracy, and increased flexibility compared to traditional methods. However, since machine vision is a precise and efficient data collector, specialized assessment algorithms are required for different inspection tasks. The effective development of algorithms that are tailored to manufactured parts and error analysis holds significant importance in the context of vision-based inspection. This research project aims to establish a comprehensive collection of computer vision algorithms capable of analyzing images of circular parts to measure and inspect roundness errors and publish the data cloudily through VNC. The proposed methodology integrates an Internet of Things (IoT) architecture and leverages MQTT protocols to enable seamless data communication.

This article is organized as follows: In Section 2, relevant studies on roundness measurement and the MZC algorithm used in determining the shape of a circular form are discussed. Section 3 covers the methodology and the experimental setup and process proposed. Section 4 presents the development of 3SMVI software and the implementation algorithms for image processing. Section 5 outlines the development of a vision system calibration, and Section 6 explains the CMM approach. Section 7 provides a discussion of the results and their interpretation. Finally, in Section 8, the authors' conclusions are summarized.

2. Previous Studies in Auto-Vision of Inspection System

The two types of measurements are diametral and radial roundness [33]. Diametral measurements are made with two-point measuring tools such as calipers or micrometers, whereas radial measurements require precision spindle instruments that are both expensive and time-consuming. These studies introduced a method for evaluating roundness and cylindricity tolerances, addressing difficulties encountered by technicians and engineers, focusing on optimizing manual procedures, and improving skills [34]. Furthermore, roundness profiles with pseudo and actual diameters were evaluated, and relationship models with neural network regression based on coordinate measuring machines were developed [35]. The "roundness tolerance band" is defined by the International Organization for Standardization (ISO) as the area between two concentric circles at the same cross-section where the difference in their radii equals the roundness tolerance value. This value emphasizes the geometric roundness tolerance standard by representing the allowable range of deviation from perfect roundness in a circular object. It specifies the acceptable margin of error for the roundness of a part [13,36,37]. This study addressed four ISO 14405-1:2016 modifiers, providing simple algorithms for evaluating circularity errors and investigating the impact of measurement system strategies on these new specifications [38].

In engineering processes, the surface structure can be defined by three primary features: form errors, roughness, and waviness. Errors encompass three vital criteria essential for the assembly and connection of different parts, namely straightness, flatness, and circularity, commonly referred to as roundness. Out-of-round (OOR) indicates the disparity between the actual and measured radius at a particular point. Roundness measurement is usually based on four globally recognized reference circles discussed in ISO-GPA and ASME Y14.5(1994), such as Maximum Inscription Radial Circle (MIC), Minimum Circumscribing Circle (MCC), Minimum Zone for Circularity (MZC), and least squares circle (LSC), as addressed by [10,39–41]. The comparison of the benchmark algorithms for calculating round errors based on MCC, MIC, and MZC was shown by [42].

Likewise, this research focused on two robust cylinder fitting alignment algorithms that combined PCA, regression, and algebraic methods, as well as a PCD cylinder alignment algorithm that can handle high-percentage deviations and improve shape recognition [43,44]. This study also conducted an iterative procedure for robust circle fitting that employs Taubin's method to obtain the center and radius, as well as geometric distances to the circle, to identify and remove outliers, thereby reducing the corrupted effect on circle parameter estimates [45]. A new roundness measurement algorithm and least squares circle fit arithmetic were employed in a rapid quality detection system for electrochemically fabricated micro-holes. The findings demonstrated reliable results and high precision, meeting the requirements for quality inspection of electrochemical machining [46]. The optimal wire spark erosion machining (WSET) turning condition minimized roundness deviation and maximized material erosion rate. It produced a suitable surface for a variety of applications, with a roundness deviation of 15.51 m and a material erosion rate of 9.35 mm^3/min. These findings will be useful in the advanced fabrication of miniature products from difficult-to-machine materials such as titanium [47]. The hybrid approach evaluates circularity error using the least squares method (LSM) and probabilistic global search Lausanne (PGSL) techniques, which have been proven to be efficient and suitable computer-aided circularity measuring instruments [48]. A circular profile surface has a maximum point that is connected by a wide circle diameter, as shown in Figure 1a. The center of the circle is represented by C, and its radius can be calculated for all points. The maximum error is determined by measuring the values for the outer and inner boundaries. The inner boundary, outer boundary, and circular center are represented by xi, xo, and c, respectively, as described by [49]. The distance is measured by establishing a reference circle from the measurement data. In the case of shafts, the largest circle that can be contained within the workpiece's profile is used, known as the MIC. Conversely, the smallest circle that can just contain the profile is used for holes, referred to as the MCC. To find the roundness error, it is necessary to find a pair of concentric circles between which the narrowest annular zone, known as the MZC, can be established. The circle that minimizes the sum of the squares of the radial distances of the data points is selected as the LSC. Accurate determination of the center position and radius of the reference circle is crucial in assembly operations. The methods MIC, MCC, and MZC, along with their respective algorithms and mathematical calculations, have been previously discussed [20]. Therefore, the primary objective of this paper is to concentrate on the mathematical calculations with algorithms of the MZC technique for measuring roundness error through the aid of computer vision. Additionally, the study aims to integrate the data collected using MQTT protocols with the Internet of Things (IoT) based on Virtual Network Computing (VNC).

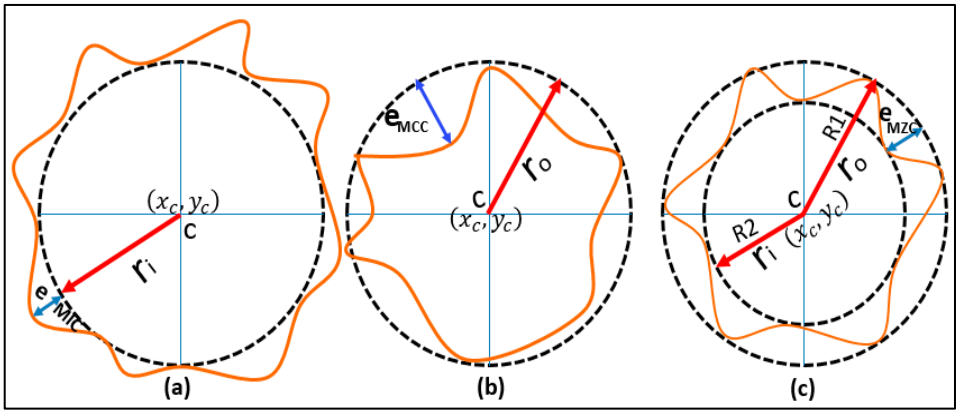

Figure 1. The fundamentals of calculating roundness using three different algorithms: (**a**) MIC, (**b**) MCC, and (**c**) MZC [50].

2.1. The Minimum Zone Circles

The MZC method determines roundness error by using two reference circles, which provide a quantitative measure by comparing the actual contour with two reference circles: the Maximum Inscribed Circle (MIC) and the Minimum Circumscribed Circle (MCC). In this technique, a circle is drawn around the circularity profile, while another circle is drawn inside the roundness profile to fit it as described by [51]. In the measurement of roundness, two circles, namely the circumscribed circle and the inscribed circle, play a crucial role. By identifying the center of these circles, which forms the minimal zone circle, the center of the measured shape is determined. This center is used as a reference point to assess the roundness profile. The roundness error is then computed by measuring the radial distance between the minimum inscribed circle and the maximum circumcised circle. The difference in radii between these circles indicates the magnitude of the roundness error present in the measured object. The roundness error is established using the MZC technique by measuring the radial separation between two circles, specifically the minimum inscribed circle and the maximum circumscribed circle. The difference in radii between these two circles indicates the roundness error of the object being measured.

$$\left\{\begin{array}{l} R_1 - R_2 \\ \sqrt{(xi - xc)^2 + (yi - yc)^2} \leq R_1 \\ \sqrt{(xi - xc)^2 + (yi - yc)^2} \geq R_2, i = 1, 2, 3, \ldots n \\ R_1 - R_2 \geq 0 \\ R_L \leq R \leq R_U; \\ x_L \leq x_c \leq x_U; \\ y_L \leq y_c \leq y_U \end{array}\right\} \quad (1)$$

where the R_1 and R_2 are the radii of $c1$ and $c2$, respectively, and thus share a center at (xc, yc). The minimum radial separation is defined as the roundness error. It is mathematically formulated as

$$e_{MZC} = R_{max} - R_{min} \quad (2)$$

In recent years, there has been a growing interest in implementing computer vision systems in industrial workplaces to detect defects in products. These systems use various image processing techniques to analyze the features and surface of the model, providing valuable information to the experts. Advanced industrial systems necessarily involve ever-improving product performance and improved product quality during the production process [52–54]. Defects, such as scratches, imperfections, or holes on the surface of the product, on the other hand, have an adverse influence mainly on the product's aesthetics and user comfort but also on its performance [55–58]. Therefore, defect detection is an efficient strategy for minimizing the environmental effects of product defects [59–61]. Machine vision in industrial processes

can help with a wide range of industrial tasks [62–64]. A typical industrial visual inspection system is categorized into three components: optical illumination, image acquisition, image processing, and defect detection [29,65]. The development of an automated smart system-based interpreter for detecting and measuring the surface feature of Example 1, Part 21, of ISO 14649 standard using machine vision inspection (3SMVI) is proposed in this study [66]. The 3SMVI system will be developed in the milling machine using a camera system and lighting system [50,66]. The 3SMVI system is widely adopted as a standard tool for measuring and inspecting surfaces. This article explores the increasing use of camera systems to validate the accuracy of surface features in design and measurement. It also discusses the challenges of measuring roundness in circles using vision and validates the system based on IoT.

3. Materials and Methodology

3.1. Materials

The CAD model displayed in Figure 2 is utilized to determine the surface area of the side view layout. The model illustrates the presence of five holes that require inspection, and the inspection circles comprise the largest portion of the model's surface area that can measure the outer edge surface. Machining parameters for a mild Delrin workpiece that has round holes with a 30 mm diameter, a spindle speed of 2000 revolutions per minute (rpm), a feed rate of 0.1 mm per revolution (mm/rev), a cutting depth of 20 mm, and a cutting speed of 250 m per second (m/s) are given. In this study, the inspection hardware is developed with the aid of IoT support devices, including a Raspberry Pi, multiple subsystem cameras, a lighting system, and a Wi-Fi router. The hardware component specifications used in the IoT configuration are listed in Table 1.

Table 1. Characteristics of parameters, hardware, and software components.

Machine Characteristics	Parameter	Specification
Machine Part	Workpiece	Delrin
	Size	120 × 100 × 50 mm
Machining	Feed rate	0.1 mm
	Spindle speed	2500 rpm
	Depth of cut	22 mm
	One Circle diameter	30 mm
	Cutting speed	250 m/s
Cutting tool	Material type	High-speed steel
	Diameter	0.6 mm
	Number of flutes	2
	Tool type	New tool
	Number of axes	Three axes, X, Y, and Z
CMM measurement	Machine type	MITUTOYO QM-353
	Resolution	0.0005 mm (0.00002 in.)
	High accuracy	Accuracy of min 0.0017 mm
	Versatility	Wide range of probe systems are available
Software		
Open CV		Open Vision Library2011, windows 10
Python		3.8.3
Pycharm editor		IDE used in computer programming for Python
CAD design		CATIA v5, R21 2020
Operating System		The Raspbian Debian Buster
MQTT protocol		Messaging protocol designed for low-bandwidth

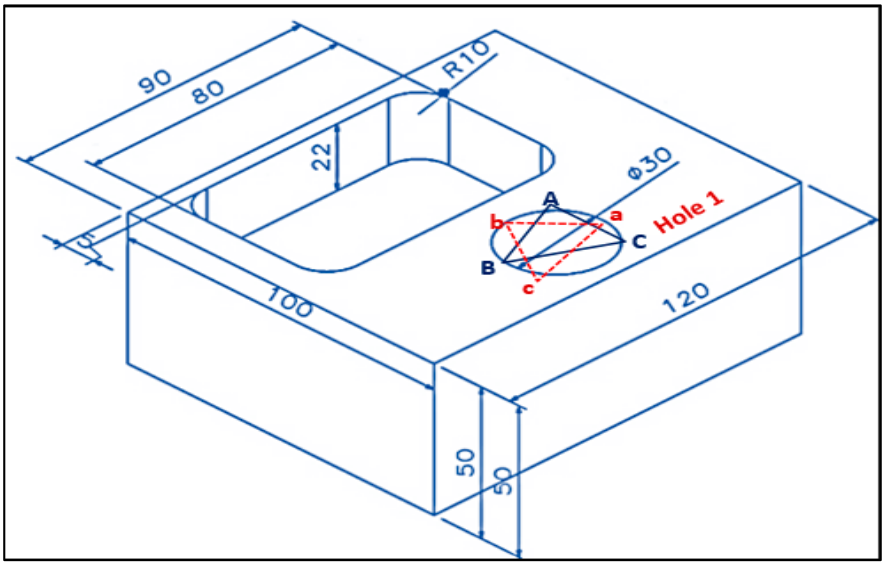

Figure 2. The CAD Design of STEP-NC file 14649 Part 21.

3.2. The Experimental Setup and Procedure

The setup for the experiment includes a combination of hardware and software for carrying out non-contact roundness tests through a vision system. Proper lighting is essential for acquiring good-quality images of the test objects. The workpiece is rotated through the use of a servo motor, while the encoder response on the fixed axis measures the angle of rotation. Simultaneously, a COMS camera captures visual data of the targeted region. The experimental setup for the Smart System-based STEP-NC file-21 for the Machine Vision Inspection (3SMVI) prototype, which incorporates cloud-based MQTT connectivity, is depicted in Figure 3. This system was implemented on an INTELITEK PROLIGHT three-axis milling machine, designed in accordance with Example 1, Part 21, of the ISO 14649 standard.

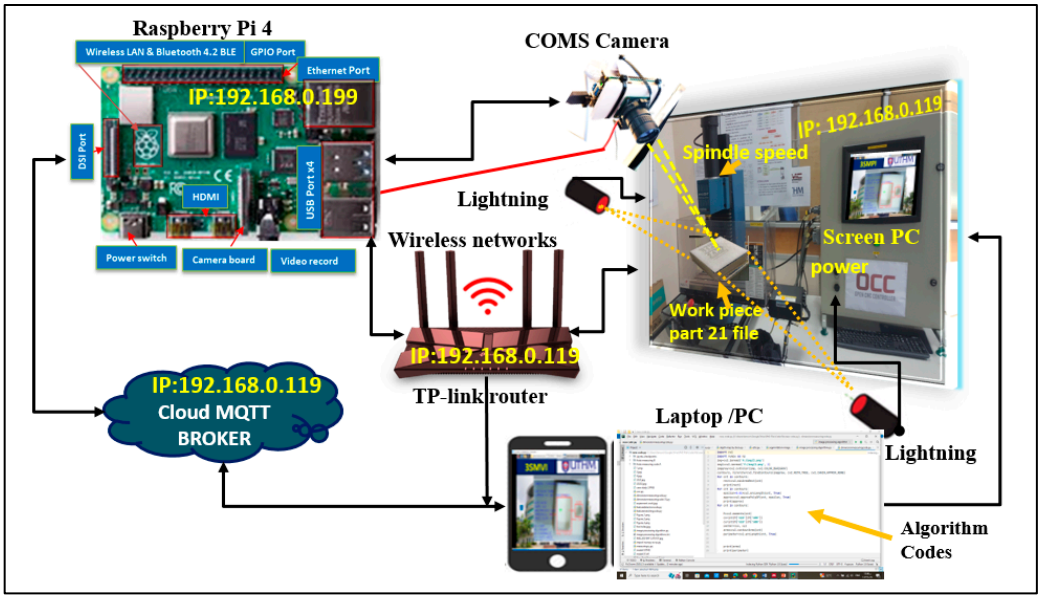

Figure 3. The 3SMVI prototype based on MQTT.

Case Study

Based on the ISO 14649 standard's Example 1, Part 21, a system design was formulated specifically for the INTELITEK PROLIGHT 3-axis milling machine. The CAD model was utilized to identify the surface region of the side view layout, with a specific focus on one hole and one pocket that necessitate inspection. The selected circle designated for inspection represents the most critical section of the model area, ensuring precise measurement of the outer surface of the edge.

This case study provides comprehensive information regarding the machining parameters employed for a Delrin prismatic mill workpiece. Notably, the workpiece has a roundness hole with a diameter of 30 mm. The specified parameters consist of a spindle speed of 2000 rpm, a feed rate of 0.1 mm/rev, a depth of cut of 20 mm, and a cutting speed of 250 m/s. To further elaborate, this case study encompasses an expanded version of Example 1 ISO 14649 Part 21 file, incorporating four holes and one pocket, as illustrated in Figure 2. Additionally, Table 1 presents an overview of the characteristic parameters, hardware, and software components involved in the study.

4. The Development of 3SMVI Software and Integration

The successful integration of machining and inspection capabilities within a single CNC machine marked a significant advancement in the establishment of the 3SMVI (Smart System-based STEP-NC file-21 for Machine Vision Inspection) system. Its primary goal is to create 3SMVI applications that combine software and hardware, as noted in [66]. The 3SMVI system is intended to operate in an IoT environment based on the STEP-NC protocol, with a heavy emphasis on hardware and software integration. The OpenCV library and Python programming language were employed to construct the machine vision system, while the 3SMVI application consisted of four major components: data diffusion mechanism, operational modules, data model, and computational intelligence algorithm. The 3SMVI system provides a comprehensive solution for machining and inspection tasks by integrating these components into a single computer. The software for the 3SMVI system was written in Python 3.8.3 with the PyCharm editor, which supported 64-bit Windows applications. It includes several computer vision and image processing algorithms for accurately measuring and inspecting roundness errors in circular components.

Figure 3 depicts the 3SMVI system based on MQTT protocols with virtual network computing. The object is placed on the backlighting table to begin the measurement or inspection process, and the capturing software, which is based on Open Computer Vision, captures and saves an image in BMP format. The vision inspection system then opens the captured image and performs the necessary inspection and measurement procedures.

4.1. The 3SMVI Hardware and Software Integration

The advancement of a smart system with interpreted files of STEP-NC for machine vision inspection based on an IoT environment. This innovation successfully integrated the machining and inspection of the roundness of the milled workpiece into a PC CNC machine cloud platform under an Open CV environment depending on a new technology approach known as IoT. Every device and machine vision were connected to the internet via the same IP address and communicated wirelessly. Therefore, the IoT application approach enables inspection integration and communication through the server broker. In addition, the information from interpreted files of the STEP-NC-based CNC machine was sensed through the camera device and finally sent back the inspection dataset into the server cloud to the STEP-NC-based IoT application. Figure 4 illustrates the smart system for interpreted files of STEP-NC for machine vision inspection based on IoT or the 3SMVI systems with the integration of both 3SMVI hardware and 3SMVI software. Additionally, the developed system provides an advanced human–machine interface that uses visual network computing (VNC) on any smart device, such as a mobile phone, tablet, and PC, through a single IP address.

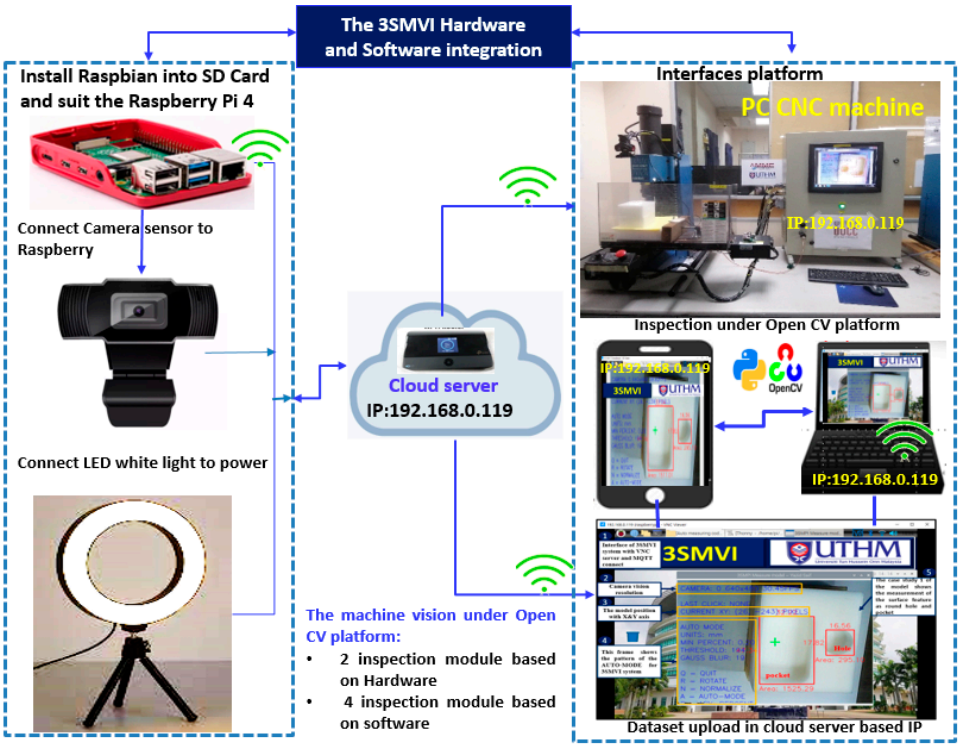

Figure 4. The integration of 3SMVI hardware- and software-based IoT.

4.2. Software Utilization and Algorithms

The data was implemented and published in cloud server-based MQTT on IoT applications. Hence, the captures of the images were data acquisition, facilitating data integration and communication during machining between inspection systems and VNC cloud servers through IoT-based technology. The main interface, as shown in Figure 5, requires two inputs from the user to carry out the measurement and inspection procedures. The 3SMVI system takes two inputs for measuring and inspecting circular objects. The diameter of the object is the first input, which is used to calibrate the system. The second input, which is used for inspection, is the maximum allowable roundness error value. To perform measurement and inspection procedures, the system employs a variety of algorithms based on computer vision and image processing.

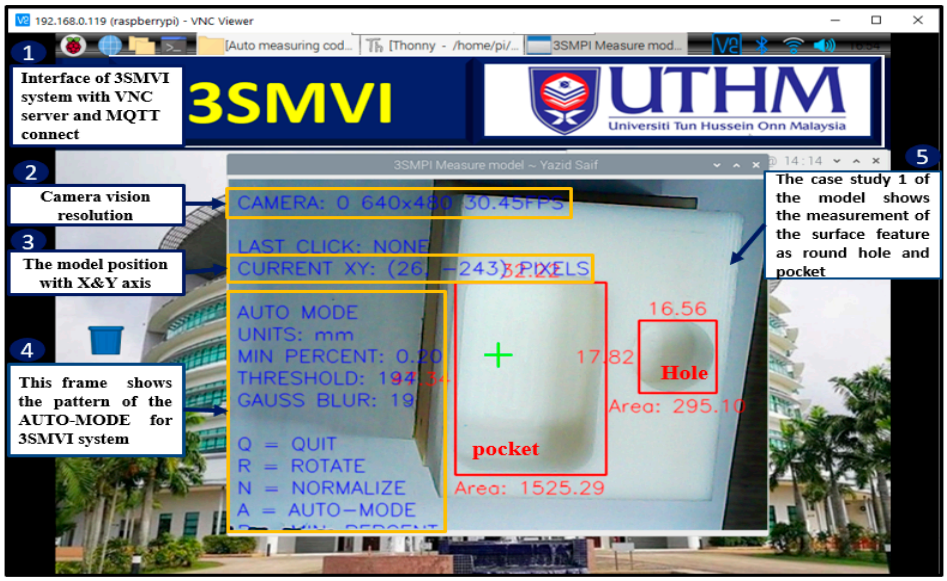

Figure 5. The 3SMVI main interface system.

4.3. Image Analysis and Segmentation

Image analysis is the initial stage of the process of image segmentation in the computer vision process. The image is fed into the system, and features are then extracted from it. Pixels that have similar characteristics are grouped together into an area, and regions with linear structures and 2D shapes are separated based on the success or failure of the computer vision-based process that relies on efficient segmentation. Industrial machine vision is one example of a typical application where the assembly of gadgets is monitored, and objects are automatically recognized and tracked. Apart from that, image segmentation has been used in traffic control, content-based image retrieval, video investigation, and sports arenas. The process of extracting meaningful information and insights from images is referred to as image analysis.

In the segmentation process, the system uses either of two features of an image separation procedure that relies on controlling the direction of illumination as part of the discontinuity. There are defined mechanisms like thresholding, region splitting and merging, and region growth used in the similarity approach to partition the image into comparable areas. Thresholding is used to separate the foreground from the background by selecting a threshold value. A binary image is generated from the gray-level image, with the threshold value being the average value of all pixels. Binary images have the advantage of minimizing data complexity and simplifying the process of image recognition and segmentation, but setting a threshold value can be difficult due to its sensitivity to noise. Clustering is the process of categorizing objects based on their characteristics. Following segmentation, models are extracted using edge detection algorithms such as Canny edges, as illustrated in Figure 10.

The process of measuring the roundness error of a Delrin workpiece involves capturing images, isolating the edge pixels of the object, and applying an edge detection algorithm. Typically, the frame grabber captures color images. However, for this particular application, binary images featuring only two colors, black and white, are required. To achieve this, a gray image must first be generated from the color image using the following formula:

$$Gl = 0.299Rc + 0.587Gc + 0.114Bc \tag{3}$$

where Gl describes the pixel's grey level and Rc, Gc, and Bc are the red, green, and blue components of the pixel color, respectively. Then, the histogram of each gray level is determined to compute a threshold value using the following:

$$T = Abs((Gl_{max}1 - Gl_{max}2)/2) \tag{4}$$

where $Gl_{max}1$ and $Gl_{max}2$ are the two grey levels with the highest frequencies, and T is the threshold value. All pixels with grey levels above the threshold are converted to black pixels to generate the binary image, and all other pixels are converted to white pixels.

4.4. An Algorithm for Detecting Edges

The edge detection process entails detecting the pixels that form the edges in a binary image. This is achieved through the use of an edge detection algorithm that compares the color of each pixel in the binary image with that of its eight neighboring pixels. If a pixel's color is black (0), and any of its neighboring pixels are white (255), it is classified as an edge pixel. However, if the pixel's color is not black or its neighboring pixels are not white, it is considered a background pixel. A process flowchart depicting these algorithms is shown in Figure 6, and further descriptions of these algorithms are provided in the subsequent sections. The following code can be used to implement this algorithm, as shown in Supplementary File.

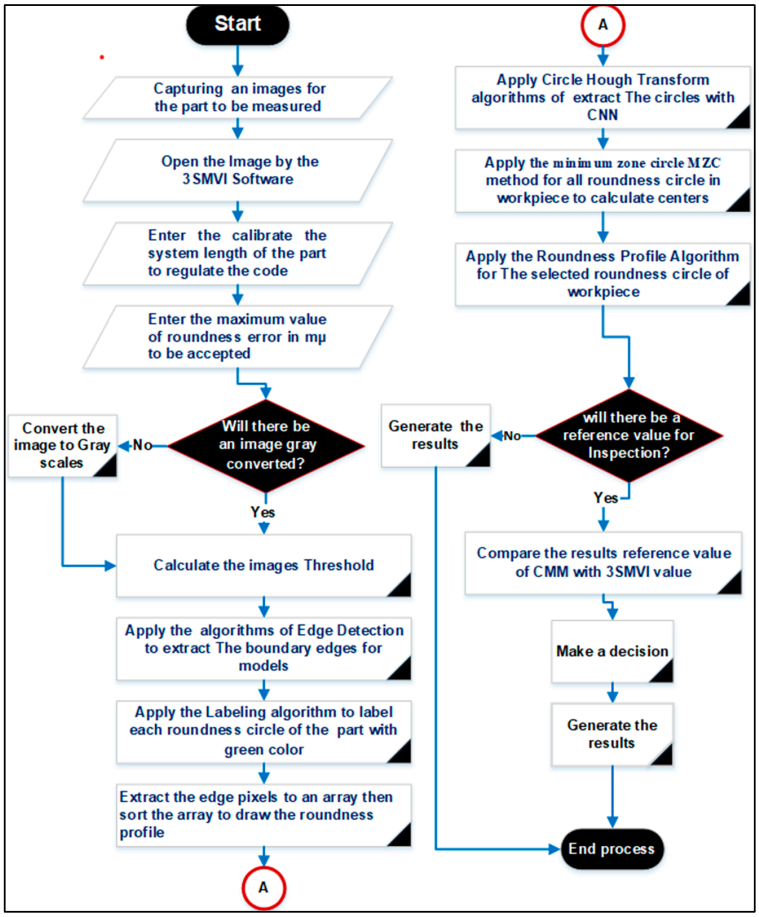

Figure 6. The 3SMVI algorithms process diagram.

Objects or Models Detection

An outline of object detection is seen in Figure 7, which includes a set of two images. Image 1 contains an object's reference, and Image 2 transforms them to grey, adds a bit of filtering to blur the image, and then subtracts the images to a binary or black-and-white image. Finally, the outcome was dilated to merge some of the near pixels or blobs, detecting the largest circle and rectangular blob around it. That was one method of detecting changes in the pixel value of images. Hence, the principle of whether to adjust a bit more behind motion or object detection to improve the final output to suit the circumstances of the image, etc. Firstly, users would need to create a video stream. Once the users have created a video feed, the first image is captured in the same way as Image 1 and used as a reference image, and then the frames are compared with the reference frame.

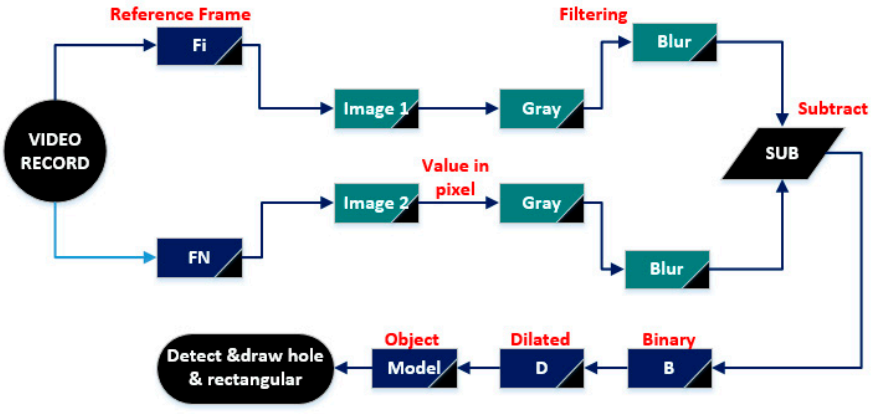

Figure 7. The framework of models with object detection.

4.5. Data Acquisition

This non-contact roundness measurement method automatically generates data acquisition by rotating the workpiece at a specific point using a machine vision system and capturing images with a high-end webcam camera placed directly in front of the object with 90 degrees of freedom. For one cycle of the measurement part, 330 images of the target region were captured, with each measurement performed after rotating the workpiece by 1.8 degrees using an Arduino-controlled two-phase stepper motor, which provides higher resolution due to its smaller step angle and usable torque. The application connects to MQTT clients over the internet by specifying the client's IP address and port number through visual network computing. Once connected, the VNC module displays the image file and serves as the primary interface for the machine vision platform. A sample image obtained from the vision system is shown in Figure 6.

Table 2 presents the surface feature of a hole pocket with four circle hole diameter values, namely 22 mm, 22 mm, 22 mm, and 22 mm, generated at different angles ranging from 0 degrees to 360 degrees in the 3SMVI vision system. The average circular error in micrometers for each hole was also calculated.

Table 2. The diameter values from the vision system for mild Delrin workpiece.

Image No.	Angle in Degree	Mild Delrin Dia. 30 mm
1	0°	29.9383
2	31°	29.9397
3	62°	29.9378
4	93°	29.9292
5	124°	29.9364
6	155°	29.9281
7	186°	29.9368
8	217°	29.9311
9	248°	29.9315
10	279°	29.9299
11	310°	29.9324
12	360°	29.9308
Roundness Circle Hole	***Error in* µm** $= Rc_{max} - Rc_{min}$	**2.9 µm**

4.6. The Algorithm for Edge Labelling

To compute the roundness error of each circular part individually, it is necessary to first identify the edge pixels of each part from the captured images. This can be achieved through the use of an edge labeling algorithm, which generates a labeled image from the edge image and assigns a unique color label to the pixels of each circular part. The algorithm follows a general process described in the reference and comprises several steps [43], including the following steps:

1. The edge-pixel image is encoded using the run-length algorithm;
2. After scanning the runs, each run is given a preliminary label. The label equivalent is then entered into a local equivalent table;
3. The classes that are resolved have equivalence;
4. Finally, based on the resolved equivalence classes, the runs are given labels.

4.7. The Error Algorithm for Roundness Holes

The roundness error algorithm, which is explained in Section 2.1, uses the minimum zone circles technique and includes the following steps:

1. The labeled image is scanned from left to right and top to bottom. During this process, the (x, y) coordinates of the edge pixels of a selected part (color) are extracted and stored in an array known as Edge Pixels;
2. The minimum zone method is then applied to the pixels in the Edge Pixels array to determine the center and radius of the minimum zone circle;
3. The center of the minimum zone circle is calculated, and the distances between this center and all pixels in the Edge Pixels array are computed. The minimum and maximum distances are identified as R_{min} and R_{max}.

5. System Calibration

To calibrate the system, it is necessary to compute the pixel sizes in both the x and y directions based on the actual size of the holes in the workpiece being measured. Camera calibration involves determining internal parameters like focal length and correcting lens distortions, as well as establishing the camera's position and orientation. This process, aided by specialized software and calibration targets, enhances measurement accuracy and computer vision applications, especially in robotics, augmented reality, and industrial quality control. The following steps are involved in this process:

1. The user provides the 3SMVI platform with the actual diameter (in millimeters) of the object being measured. If the object is comprised of multiple circular parts, the outer part's size (maximum diameter) should be utilized.
2. The software searches for the two edge pixels on the outer contour with the minimum and maximum x coordinates to determine the maximum diameter of the captured image in the x direction ($D_{max}x$) using the formula

$$D_{max}x = Abs(X_{max} - X_{min}) \tag{5}$$

   where X_{max} and X_{min} are the maximum and minimum x coordinates of the edge pixels of the outer contour, respectively.
3. The calibration factor in the x direction (CFx) is calculated as follows:

$$CFx = Dactual / D_{max}x \tag{6}$$

4. In the same manner, the calibration process also involves determining the calibration factor in the y direction (CFy) by identifying the two pixels with the minimum and maximum y coordinates, which can be obtained by using the formula

$$CFy = Dactual / D_{max}y \tag{7}$$

5. After calculating CFx and CFy, all x and y coordinates of the edge pixels are multiplied by these calibration factors.
6. The primary roundness error $(RE\ primary)$ is then calculated using the least squares circle technique on the edge pixels.
7. Furthermore, using a formula derived from Excel, the fixed error (FE) in pixels is determined based on the user-provided value of the smoothing factor (SF).
8. The fixed error is then calibrated and expressed in millimeters ($FE\ mm$) using the following equation:

$$FE\ mm = FE\ pixel\ CFx \times CFy \tag{8}$$

9. The final roundness error $(RE\ final)$ is calculated as follows:

$$RE\ final = RE\ primary - FE\ mm \tag{9}$$

Camera-to-Workpiece Distance Estimation

After calibration, the distance to the object was calculated using a single photograph. Thus, the concept of the given solution was the image analysis resulting from the object moving away from the point for which it defined the focus, how to use a single camera to figure out the distance to an object, where the focal distance (f) and height (h) and distance the distance between the object and the lens known as (d). b was the height, while m was the distance between the camera and a and b, which was named the reflection of height. Figure 8 below shows the points between the camera distance and the object.

$$\frac{a}{f} = \tan\theta_1 = \frac{h}{d} \tag{10}$$

$$\frac{b}{f} = \tan\theta_2 = \frac{h}{d-m} \tag{11}$$

By dividing Equations (10) and (11), they may represent the distance between the object and lens and calculate the pixel distance to figure out the length.

$$\begin{gathered} \Rightarrow \frac{a}{b} = \frac{\tan\theta_1}{\tan\theta_2} = \frac{h}{d} \times \frac{d-m}{h} = 1 - \frac{m}{d}; \\ \Rightarrow \frac{m}{d} = 1 - \frac{a}{b}; \\ \Rightarrow d = \frac{m}{1-\frac{a}{b}} \end{gathered} \tag{12}$$

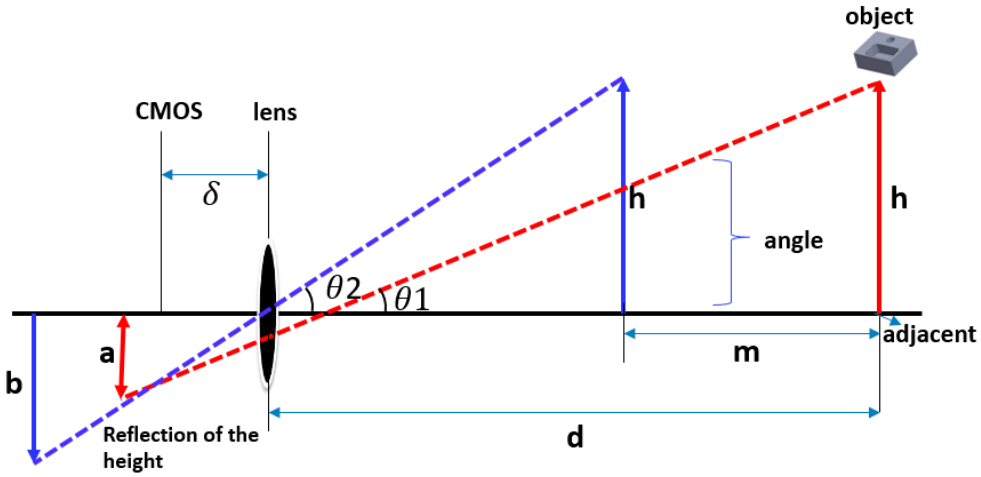

Figure 8. The camera-to-workpiece distance estimation.

6. CMM Inspection of Contact Measurement

In this validation section, a case study was used to inspect the roundness of a circle hole known as an offline coordinate measuring machine. Figure 9 shows the illustration of a model that measures the surface feature during the inspection process using the CMM technique, as described in this section. Furthermore, the research employed an offline measuring tool to evaluate the Delrin components utilizing Example 1, Part 21, file based on the STEP-NC environment. The QM-353 manual CMM equipment at UTHM Metrology was used to examine samples of the same workpiece holes. The CMM measurements were conducted in a particular sequence to determine the roundness of the holes and surface characteristics of mild Delrin workpieces.

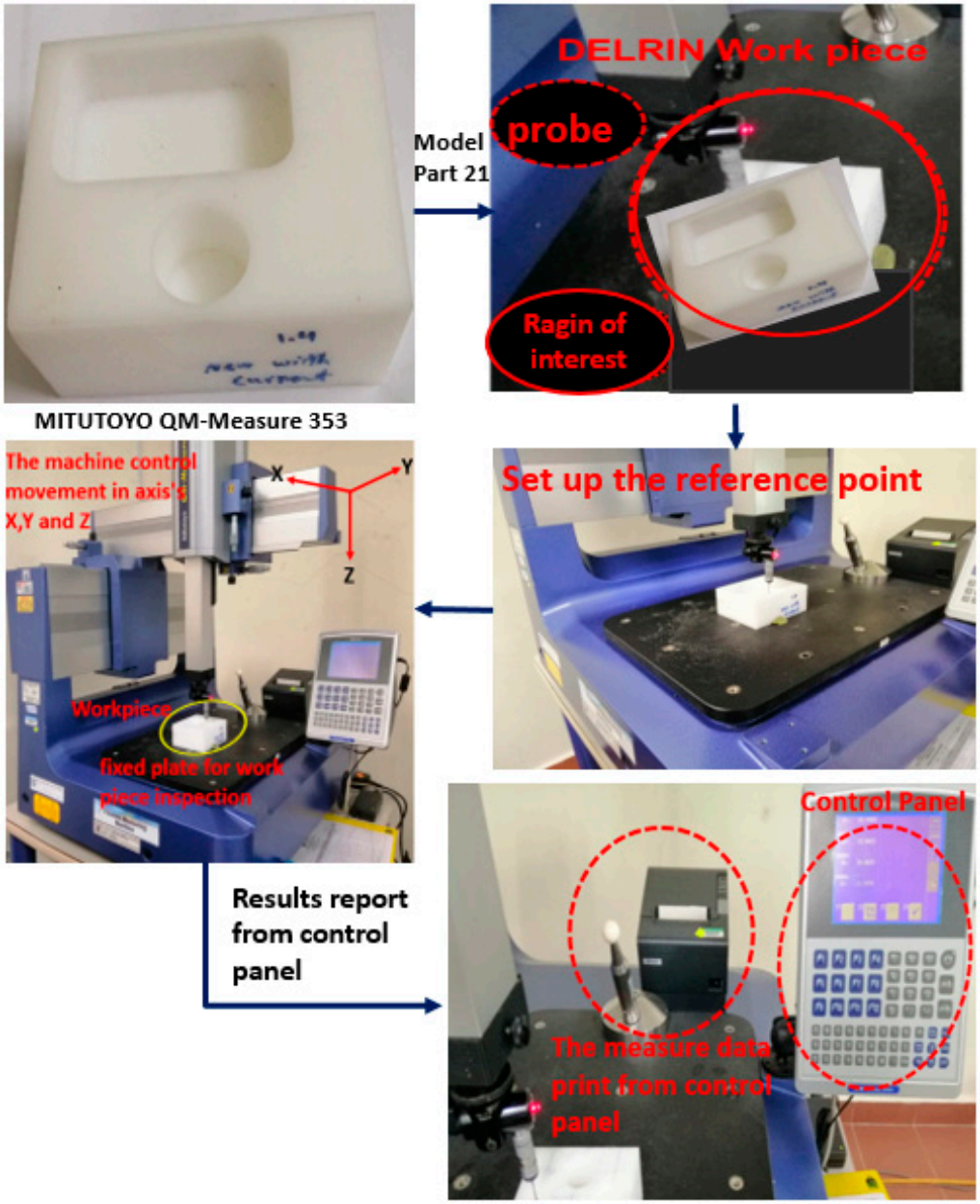

Figure 9. The CMM implementation for Case Study 1.

7. Result and Discussion

The study utilized a new cutting tool to produce Delrin parts with the Example 1, Part 21, file based on the STEP-NC environment using a PROLIGHT CNC milling machine in this validation section. However, the inspection processes utilizing image processing techniques remained the same as described in the previous section on the 3SMVI system implementation. Figure 10 depicts a graphical representation of the inspection procedure, illustrating the steps involving image processing, image analysis, and computational intelligence for measurement identification. Images were pre-processed to identify their contents for further analysis, such as counting or measuring roundness circles and plane surface features. When identifying objects in an image, edges play a crucial role. Boundaries were the lines that differentiate groups of identical pixels in the image from groups of distinct pixels. The edge considers image pixels that delineate the boundary of a target, such as whether the image's background finishes and the image continues.

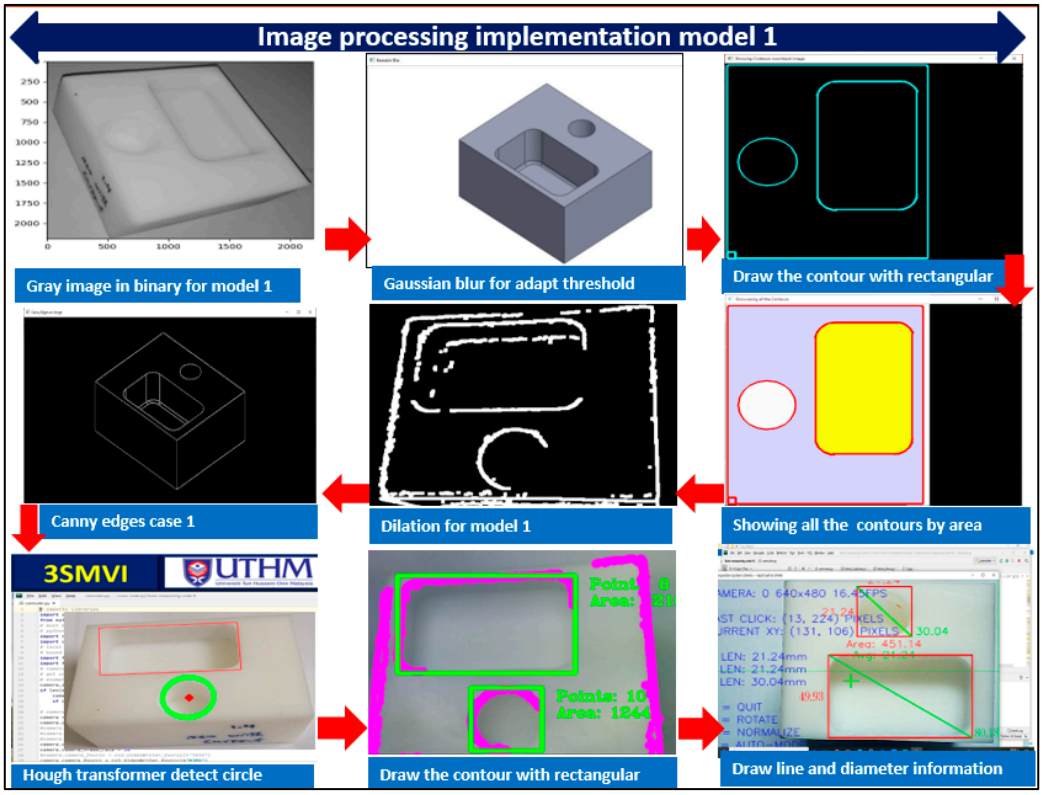

Figure 10. Implementation of image processing technique for Case Study 1.

Table 2 illustrates the surface feature diameter of the roundness circle values of Example 1, Part 21 file based on ISO 14649, developed using the 3SMVI vision system in twelve points. Consequently, Figure 11 displays consistent and predictable diameter data at each point, covering various angles ranging from zero degrees to 360 degrees of position. In addition, it depicted the data in red color decrease as the minimum value in three measurements.

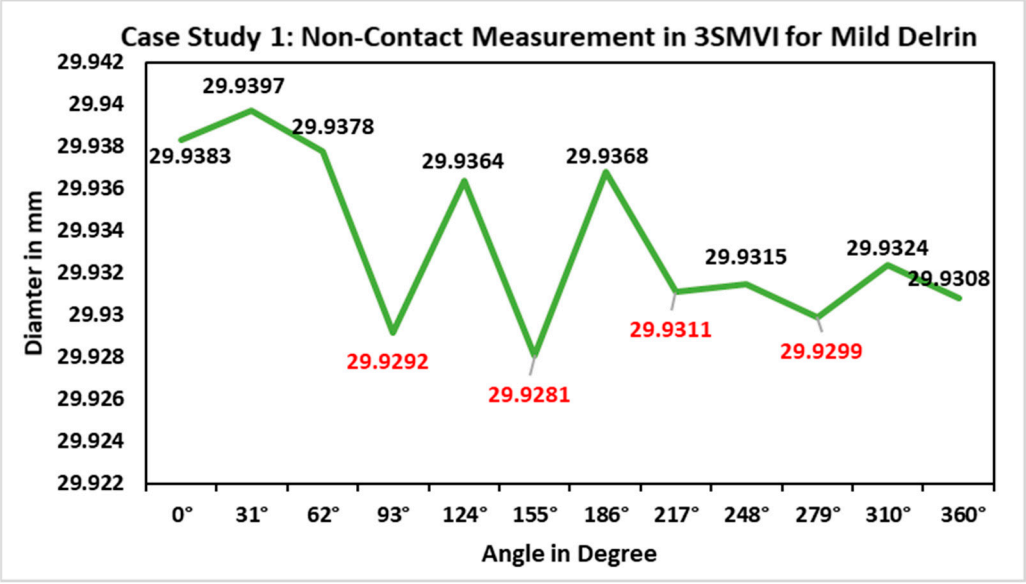

Figure 11. Case study with non-contact measurement in 3SMVI for mild Delrin.

Table 3 presents the results of the measurements taken with the MITUTOYO QM-Measure CMM of the surface feature of a roundness hole of the workpiece. Figure 12 shows that the diameter data obtained at each point were uniform and predictable, with positions ranging from 0° to 360°. The red data points represented the minimum value measurements, which were considered the optimal values for the vision system. However, while the contact approach provided accurate results, it was more time-consuming compared to the vision system. The main issue with the contact method was the wear and tear that occurred between the measuring probe and the workpiece.

Table 3. Dimensional information from the CMM for a mild Delrin workpiece.

No. of Point	Points	Mild Delrin Dia. 30 mm
3	A,B,C	30.0121
3	A,C,B	30.0099
3	B,A,C	30.0112
3	B,C,A	30.0123
3	C,A,B	30.0133
3	C,B,A	30.0113
3	a,b,c	30.0104
3	a,c,b	30.0109
3	b,a,c	30.0124
3	b,c,a	30.0116
3	c,a,b	30.0128
3	c,b,a	30.0103

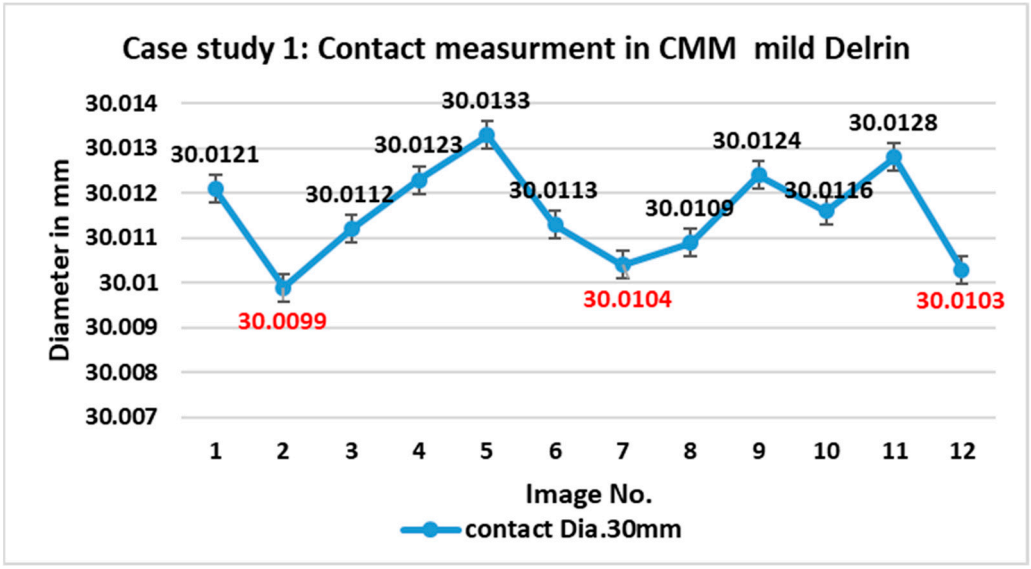

Figure 12. CMM of contact measurement for mild Delrin workpiece in Case Study 1.

Table 4 illustrates the average value of the difference errors in microns between contact and non-contact measurements of the dimensions in each parameter for the case study. Therefore, Figure 13 shows the decline of deference errors in microns between the 3SMVI and CMM.

Table 4. Comparison of the difference of average circle hole error between 3SMVI and CMM measurements for mild Delrin Case Study 1.

Diameter in mm	Hole Circle Error from 3SMVI System in µm	Hole Circle Error from CMM in µm	Difference in µm
30	11.6 µm	2.9 µm	8.7

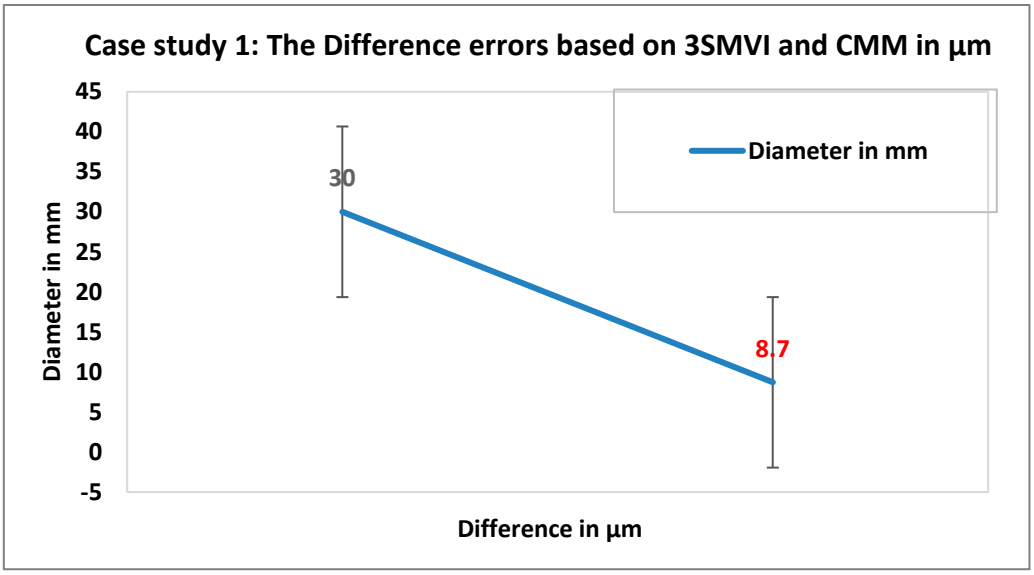

Figure 13. The difference error based on 3SMVI and CMM in µm.

8. Conclusions and Future Research

The fusion of IoT architecture, computer vision, and image processing methods has driven progress in measuring roundness within industrial automation. This integration enhances the accuracy and effectiveness of assessing roundness in industrial applications. IoT architecture facilitates real-time data exchange among devices, enabling instant monitoring and analysis of roundness measurements. This interconnectedness enables automated systems to gather and process image data from diverse sensors and cameras, offering a holistic perspective on an object's roundness.

This paper discusses the development of an intelligent system utilizing machine vision inspection within an IoT framework and ISO 14649 interpreted files. A case study, including Example 1, Part 21, of STEP-NC, validated the system's functionality and confirmed its high accuracy compared to previous models. The article stresses the significance of assessing uncertainty from the perspective of the MVIS system rather than solely focusing on algorithm development. The 3SMVI system, built on IoT architecture, has been fully developed, and the next step involves integrating advanced intelligent algorithms to enhance its capabilities. The primary contribution of this research is the examination of workpiece roundness using the 3SMVI system within an IoT and CMM framework. The IoT architecture facilitates seamless communication between the roundness measurement system and connected devices, enabling efficient data exchange, remote monitoring, and data-driven decision-making.

Computer vision algorithms play a crucial role in extracting meaningful information from the captured images. These algorithms can identify and analyze geometric features, enabling accurate roundness measurements. Through the use of edge detection, contour analysis, and shape-fitting algorithms, the system can precisely determine the roundness of objects with minimal human intervention. A vision system was introduced to measure and inspect circular parts' roundness errors using a non-contact method that adheres to geometric roundness tolerance standards. The 3SMVI system was developed to assist measurement and inspection processes by analyzing captured images using image processing and computer vision algorithms based on Open Computer Vision. Therefore, to ensure the system's accuracy, the roundness error of holes in workpiece parts was measured using both a coordinate measuring machine (CMM) and the machine vision inspection system (MVIS). The results were compared, and the maximum difference between the outcomes of the two systems was found to be 8.7%.

In a future study, we aim to enhance the 3SMVI system's performance by upgrading hardware and software algorithms, improving image quality, and using more protocols for

information transmission via cloud computing servers. It will focus on enhancing surface feature detection and manufacturing optimization using deep learning techniques and incorporating machine learning and artificial intelligence for continuous improvement and intelligent decision-making in industrial automation.

Supplementary Materials: The following supporting information can be downloaded at: https://www.mdpi.com/article/10.3390/app132011419/s1.

Author Contributions: Conceptualization, Y.S., A.Z.M.R., A.A. and H.Q.A.A.; Methodology, Y.S., A.Z.M.R., Y.Y., M.L.A., S.A.-A. and A.A.; Software, Y.S.; Validation, M.L.A., S.A.-A., D.H.D., M.A.A.-m. and H.Q.A.A.; Formal analysis, M.L.A., S.A.-A., D.H.D. and M.A.A.-m.; Investigation, Y.Y., S.A.-A., D.H.D., A.A., Y.H.G. and H.Q.A.A.; Resources, A.Z.M.R., A.A. and M.A.A.-m.; Data curation, Y.S. and M.A.A.-m.; Writing—original draft, Y.S.; Writing—review & editing, A.Z.M.R., Y.Y., M.L.A. and Y.H.G.; Supervision, A.Z.M.R.; Funding acquisition, Y.H.G. and H.Q.A.A. All authors have read and agreed to the published version of the manuscript.

Funding: The authors would like to express their sincere gratitude to the Ministry of Higher Education (MOHE) in Malaysia for their invaluable support through the Fundamental Grant Scheme (FRGS/1/2020/STG01/UTHM/02/2). Furthermore, the authors would like to acknowledge the generous provision of facilities by the Sustainable Polymer Engineering, Advanced Manufacturing, and Material Centre (SPEN-AMMC). Moreover, this work was supported by Institute of Information & communications Technology Planning & Evaluation (IITP) grant funded by the Korea government (MSIT) (2021-0-00755), Dark data analysis technology for data scale and accuracy improvement.

Institutional Review Board Statement: Not applicable.

Informed Consent Statement: Not applicable.

Data Availability Statement: All the relevant data are within the manuscript and supporting information file as Supplementary File.

Conflicts of Interest: The authors declare no conflict of interest.

Abbreviations

ASME	American Society of Mechanical Engineers
ACO	Colony Optimization
CNC	Computer Numerical Control
CMM	Coordinate measuring machine
C	Center of this circle
CMOS	Complementary metal–oxide–semiconductor
EO	Engineering Ontology
e_{MZC}	Error-based Minimum Zone radial circles
CLIM	Closed-loop inspection manufacturing
CAIP	Computer-aided Inspection Planning
FTP	File Transfer Protocol
GA	General Assembly Simulation
GD&T	Geometric Dimensioning and Tolerance
I 4.0	The Fourth Industrial Revolution
IoT	Internet of Things
WSET	Wire spark erosion machining
ISO	International Standard Organization
LED	Light-emitting Diodes
MQTT	Message Queuing Telemetry Transport
MZC	Minimum Zone for Radial Circles
MTD	Metrology for the Digitalization
Open CV	Open Computer Vision
OLP	Offline Programming System
OOR	Out-of-the-Round
QM	Quality MITUTOYO Measure
RGB	Three channels of color: Red, Green, and Blue

R_i	Radius inner
R_U	Upper radius
R_L	Lower radius
STEP-NC	The Standard for the Exchange of Product Model Data for Numerical Control
VNC	Visual network center
3SMVI	Smart System based on interpreted STEP-NC for Machine Vision Inspection
3D	Three-dimension model

References

1. Stojadinovic, S.M.; Majstorovic, V.D.; Durakbasa, N.M. Toward a cyber-physical manufacturing metrology model for industry 4.0. *Artif. Intell. Eng. Des. Anal. Manuf.* **2020**, *35*, 20–36. [CrossRef]
2. Ahmad, M.I.; Yusof, Y.; Daud, E.; Latiff, K.; Kadir, A.Z.A.; Saif, Y. Machine monitoring system: A decade in review. *Int. J. Adv. Manuf. Technol.* **2020**, *108*, 3645–3659. [CrossRef]
3. Ashima, R.; Haleem, A.; Bahl, S.; Javaid, M.; Mahla, S.K.; Singh, S. Automation and manufacturing of smart materials in additive manufacturing technologies using Internet of Things towards the adoption of industry 4.0. *Mater. Today Proc.* **2021**, *45*, 5081–5088. [CrossRef]
4. Nate, K.; Tentzeris, M.M. A novel 3-D printed loop antenna using flexible NinjaFlex material for wearable and IoT applications. In Proceedings of the 2015 IEEE 24th Electrical Performance of Electronic Packaging and Systems (EPEPS), San Jose, CA, USA, 25–28 October 2015; pp. 171–174. [CrossRef]
5. Qin, W.; Chen, S.; Peng, M. Recent advances in Industrial Internet: Insights and challenges. *Digit. Commun. Netw.* **2020**, *6*, 1–13. [CrossRef]
6. Benbarrad, T.; Salhaoui, M.; Kenitar, S.B.; Arioua, M. Intelligent Machine Vision Model for Defective Product Inspection Based on Machine Learning. *J. Sens. Actuator Netw.* **2021**, *10*, 7. [CrossRef]
7. Pan, Y.; White, J.; Schmidt, D.C.; Elhabashy, A.; Sturm, L.; Camelio, J.; Williams, C. Taxonomies for Reasoning About Cyber-physical Attacks in IoT-based Manufacturing Systems. *Int. J. Interact. Multimedia Artif. Intell.* **2017**, *4*, 45. [CrossRef]
8. Wen, X.; Xia, Q.; Zhao, Y. An effective genetic algorithm for circularity error unified evaluation. *Int. J. Mach. Tools Manuf.* **2006**, *46*, 1770–1777. [CrossRef]
9. Renzi, C.; Ceruti, A.; Leali, F. Integrated geometrical and dimensional tolerances stack-up analysis for the design of mechanical assemblies: An application on marine engineering. *Comput.-Aided. Des. Appl.* **2018**, *15*, 631–642. [CrossRef]
10. Guu, S.M.; Tsai, D.M. Measurement of roundness: A nonlinear approach. *Proc. Natl. Sci. Counc. Repub. China Part A Phys. Sci. Eng.* **1999**, *23*, 348–352.
11. Mohamed, A.; Esa, A.H.; Ayub, M.A. Roundness measurement of cylindrical part by machine vision. In Proceedings of the International Conference on Electrical, Control and Computer Engineering 2011 (InECCE), Kuantan, Malaysia, 21–22 June 2011; pp. 486–490. [CrossRef]
12. Ayub, M.A.; Mohamed, A.B.; Esa, A.H. In-line Inspection of Roundness Using Machine Vision. *Procedia Technol.* **2014**, *15*, 807–816. [CrossRef]
13. Gadelmawla, E.; Khalifa, W.; Elewa, I. Measurement and Inspection of Roundness Using Computer Vision. *MEJ Mansoura Eng. J.* **2008**, *33*, 20–32. [CrossRef]
14. Ali, S.H.R.; Mohamd, O.M. Dimensional and Geometrical Form Accuracy of Circular Pockets Manufactured for Aluminum, Copper and Steel Materials on CNC Milling Machine Using CMM. *Int. J. Eng. Res. Afr.* **2015**, *17*, 64–73. [CrossRef]
15. Gapinski, B.; Kołodziej, A. Measurement of diameter and roundness deviation for circle with incomplete contour. In Proceedings of the 11th International Symposium on Measurement and Quality Control 2013, Cracow-Kielce, Poland, 11–13 September 2013; pp. 142–145.
16. Janusiewicz, A.; Adamczak, S.; Makieła, W.; Stpień, K. Determining the theoretical method error during an on-machine roundness measurement. *Meas. J. Int. Meas. Confed.* **2011**, *44*, 1761–1767. [CrossRef]
17. Lei, X.; Song, H.; Xue, Y.; Li, J.; Zhou, J.; Duan, M. Method for cylindricity error evaluation using Geometry Optimization Searching Algorithm. *Meas. J. Int. Meas. Confed.* **2011**, *44*, 1556–1563. [CrossRef]
18. Mears, L.; Roth, J.T.; Djurdjanovic, D.; Yang, X.; Kurfess, T. Quality and Inspection of Machining Operations: CMM Integration to the Machine Tool. *J. Manuf. Sci. Eng.* **2009**, *131*, 051006. [CrossRef]
19. Stojadinovic, S.M.; Majstorovic, V.D.; Durakbasa, N.M.; Sibalija, T.V. Towards an intelligent approach for CMM inspection planning of prismatic parts. *Meas. J. Int. Meas. Confed.* **2016**, *92*, 326–339. [CrossRef]
20. Gadelmawla, E.S. Computer Aided Measurement software for roundness evaluation from the coordinate measurement data. In Proceedings of the Ninth Cairo University International Conference on Mechanical Design and Production (MDP-9), Cairo, Egypt, 8–10 January 2008; pp. 270–285.
21. Hong, R.; Xiang, C.; Liu, H.; Glowacz, A.; Pan, W. Visualizing the Knowledge Structure and Research Evolution of Infrared Detection Technology Studies. *Information* **2019**, *10*, 227. [CrossRef]
22. Xu, P.; Guan, C.; Zhang, H.; Li, G.; Zhao, D.; Ross, R.J.; Shen, Y. Application of Nondestructive Testing Technologies in Preserving Historic Trees and Ancient Timber Structures in China. *Forests* **2021**, *12*, 318. [CrossRef]

23. Yang, J.; Li, S.; Wang, Z.; Dong, H.; Wang, J.; Tang, S. Using deep learning to detect defects in manufacturing: A comprehensive survey and current challenges. *Materials* **2020**, *13*, 5755. [CrossRef]
24. de Araujo, P.R.M.; Lins, R.G. Computer vision system for workpiece referencing in three-axis machining centers. *Int. J. Adv. Manuf. Technol.* **2020**, *106*, 2007–2020. [CrossRef]
25. de Araujo, P.R.M.; Lins, R.G. Cloud-based approach for automatic CNC workpiece origin localization based on image analysis. *Robot. Comput. Manuf.* **2021**, *68*, 102090. [CrossRef]
26. Kumar, B.M.; Ratnam, M.M. Machine vision method for non-contact measurement of surface roughness of a rotating workpiece. *Sens. Rev.* **2015**, *35*, 10–19. [CrossRef]
27. Jones, J.M.; Foster, W.; Twomey, C.R.; Burdge, J.; Ahmed, O.M.; Pereira, T.D.; A Wojick, J.; Corder, G.; Plotkin, J.B.; Abdus-Saboor, I. A machine-vision approach for automated pain measurement at millisecond timescales. *eLife* **2020**, *9*, 1–22. [CrossRef] [PubMed]
28. McCarthy, C.L.; Hancock, N.H.; Raine, S.R. Applied machine vision of plants: A review with implications for field deployment in automated farming operations. *Intell. Serv. Robot.* **2010**, *3*, 209–217. [CrossRef]
29. Di Leo, G.; Liguori, C.; Pietrosanto, A.; Sommella, P. A vision system for the online quality monitoring of industrial manufacturing. *Opt. Lasers Eng.* **2016**, *89*, 162–168. [CrossRef]
30. Fernández-Robles, L.; Azzopardi, G.; Alegre, E.; Petkov, N. Machine-vision-based identification of broken inserts in edge profile milling heads. *Robot. Comput. Manuf.* **2017**, *44*, 276–283. [CrossRef]
31. Saif, Y.; Yusof, Y.; Latif, K.; Kadir, A.Z.A.; Ahmed, M.L. Systematic review of STEP-NC-based inspection. *Int. J. Adv. Manuf. Technol.* **2020**, *108*, 3619–3644. [CrossRef]
32. Lin, E.-Y.; Tu, C.-T.; Lien, J.-J.J. Nut Geometry Inspection Using Improved Hough Line and Circle Methods. *Sensors* **2023**, *23*, 3961. [CrossRef]
33. Meadows, J.D. *Measurement of Geometric Tolerances in Manufacturing*; Marcell Dekker, Inc.: New York, NY, USA, 1998; Volume 1998.
34. García-Martínez, E.; García-González, N.; Manjabacas, M.C.; Miguel, V. Validation of a Manual Methodology for Measuring Roundness and Cylindricity Tolerances. *Appl. Sci.* **2023**, *13*, 9702. [CrossRef]
35. Zhao, Z.; Xi, J.; Zhao, X.; Zhang, G.; Shang, M. Evaluation of the Calculated Sizes Based on the Neural Network Regression. *Math. Probl. Eng.* **2018**, *2018*, 4078456. [CrossRef]
36. Cioboata, D.; Dontu, O.; Besnea, D.; Ciobanu, R.; Soare, A. Mecatronic equipment for bearing ring surface inspection. *Rom. Rev. Precis. Mech. Opt. Mechatron.* **2015**, *2015*, 262–266.
37. Du, C.L.; Luo, C.X.; Han, Z.T.; Zhu, Y.S. Applying particle swarm optimization algorithm to roundness error evaluation based on minimum zone circle. *Meas. J. Int. Meas. Confed.* **2014**, *52*, 12–21. [CrossRef]
38. Jbira, I.; Tahan, A.; Mahjoub, M.A.; Louhichi, B. Evaluation of the Algorithmic Error of New Specification Tools for an ISO 14405-1:2016 Size. In *International Design Engineering Technical Conferences and Computers and Information in Engineering Conference, Quebec City, QC, Canada, 26–29 August 2018*; American Society of Mechanical Engineers: New York, NY, USA, 2018. [CrossRef]
39. Gosavi, A.; Cudney, E.A. Form Errors in Precision Metrology: A Survey of Measurement Techniques. *Qual. Eng.* **2012**, *24*, 369–380. [CrossRef]
40. Kshaurad, K.; Kiran, M.; Shanmuganatan, S. Minimum zone tolerance algorithm to detect roundness error for machined rods using vision system. *Mater. Today Proc.* **2021**, *46*, 5997–6003. [CrossRef]
41. Sui, W.; Zhang, D. Four Methods for Roundness Evaluation. *Phys. Procedia* **2012**, *24*, 2159–2164. [CrossRef]
42. Rhinithaa, P.T.; Selvakumar, P.; Sudhakaran, N.; Anirudh, V.; Lawrence, K.D.; Mathew, J. Comparative study of roundness evaluation algorithms for coordinate measurement and form data. *Precis. Eng.* **2018**, *51*, 458–467. [CrossRef]
43. Nurunnabi, A.; Sadahiro, Y.; Lindenbergh, R. Robust cylinder fitting in three-dimensional point cloud data. *Int. Arch. Photogramm. Remote Sens. Spat. Inf. Sci.-ISPRS Arch.* **2017**, *42*, 63–70. [CrossRef]
44. Nurunnabi, A.; Sadahiro, Y.; Laefer, D.F. Robust statistical approaches for circle fitting in laser scanning three-dimensional point cloud data. *Pattern Recognit.* **2018**, *81*, 417–431. [CrossRef]
45. Guo, J.; Yang, J. An iterative procedure for robust circle fitting. *Commun. Stat.-Simul. Comput.* **2019**, *48*, 1872–1879. [CrossRef]
46. Liu, Y.; Zhu, L.S.; Xiong, Q.J. Development of Quality Detecting System for Micro Holes by ECM Based on Machine Vision Technology. *Appl. Mech. Mater.* **2013**, *397–400*, 1482–1485. [CrossRef]
47. Chaubey, S.K.; Gupta, K. An experimental study on out-of-roundness and material erosion rate during wire spark erosion turning of titanium cylindrical bars. *J. Mater. Res. Technol.* **2023**, *24*, 7539–7551. [CrossRef]
48. Srinivasu, D.S.; Venkaiah, N. Minimum zone evaluation of roundness using hybrid global search approach. *Int. J. Adv. Manuf. Technol.* **2017**, *92*, 2743–2754. [CrossRef]
49. Liu, Q.M.; Li, X. Machine Vision Detection on Circle with Non-Uniform Points. *Appl. Mech. Mater.* **2014**, *687–691*, 819–822. [CrossRef]
50. Saif, Y.; Yusof, Y.; Latif, K.; Kadir, A.Z.A.; Ahmed, M.B.L.; Adam, A.; Hatem, N.; Memon, D.A. Roundness Holes' Measurement for milled workpiece using machine vision inspection system based on IoT structure: A case study. *Meas. J. Int. Meas. Confed.* **2022**, *195*, 111072. [CrossRef]
51. Sun, T.-H. Applying particle swarm optimization algorithm to roundness measurement. *Expert Syst. Appl.* **2009**, *36*, 3428–3438. [CrossRef]
52. Wang, T.; Chen, Y.; Qiao, M.; Snoussi, H. A fast and robust convolutional neural network-based defect detection model in product quality control. *Int. J. Adv. Manuf. Technol.* **2018**, *94*, 3465–3471. [CrossRef]

53. Liao, Z.; Abdelhafeez, A.; Li, H.; Yang, Y.; Diaz, O.G.; Axinte, D. State-of-the-art of surface integrity in machining of metal matrix composites. *Int. J. Mach. Tools Manuf.* **2019**, *143*, 63–91. [CrossRef]
54. AKim, D.-H.; Kim, T.J.Y.; Wang, X.; Kim, M.; Quan, Y.-J.; Oh, J.W.; Min, S.-H.; Kim, H.; Bhandari, B.; Yang, I.; et al. Smart Machining Process Using Machine Learning: A Review and Perspective on Machining Industry. *Int. J. Precis. Eng. Manuf.-Green Technol.* **2018**, *5*, 555–568. [CrossRef]
55. Bulnes, F.G.; Usamentiaga, R.; Garcia, D.F.; Molleda, J. An efficient method for defect detection during the manufacturing of web materials. *J. Intell. Manuf.* **2016**, *27*, 431–445. [CrossRef]
56. Song, K.; Yan, Y. A noise robust method based on completed local binary patterns for hot-rolled steel strip surface defects. *Appl. Surf. Sci.* **2013**, *285*, 858–864. [CrossRef]
57. Zhang, Y.; Shen, H.; Bo, X.; Li, A.; Zhan, Y.; Gu, H. Amultiscale evaluation of the surface integrity in boring trepanning association deep hole drilling. *Int. J. Mach. Tools Manuf.* **2017**, *123*, 48–56. [CrossRef]
58. Rao, X.; Zhang, F.; Lu, Y.; Luo, X.; Chen, F. Surface and subsurface damage of reaction-bonded silicon carbide induced by electrical discharge diamond grinding. *Int. J. Mach. Tools Manuf.* **2020**, *154*, 103564. [CrossRef]
59. Huang, S.-H.; Pan, Y.-C. Automated visual inspection in the semiconductor industry: A survey. *Comput. Ind.* **2015**, *66*, 1–10. [CrossRef]
60. Ravimal, D.; Kim, H.; Koh, D.; Hong, J.H.; Lee, S.-K. Image-Based Inspection Technique of a Machined Metal Surface for an Unmanned Lapping Process. *Int. J. Precis. Eng. Manuf. Technol.* **2020**, *7*, 547–557. [CrossRef]
61. Ren, Z.; Fang, F.; Yan, N.; Wu, Y. State of the Art in Defect Detection Based on Machine Vision. *Int. J. Precis. Eng. Manuf.-Green Technol.* **2021**, *9*, 661–691. [CrossRef]
62. Penumuru, D.P.; Muthuswamy, S.; Karumbu, P. Identification and classification of materials using machine vision and machine learning in the context of industry 4.0. *J. Intell. Manuf.* **2020**, *31*, 1229–1241. [CrossRef]
63. Ali, M.A.H.; Lun, A.K. A cascading fuzzy logic with image processing algorithm–based defect detection for automatic visual inspection of industrial cylindrical object's surface. *Int. J. Adv. Manuf. Technol.* **2019**, *102*, 81–94. [CrossRef]
64. Badmos, O.; Kopp, A.; Bernthaler, T.; Schneider, G. Image-based defect detection in lithium-ion battery electrode using convolutional neural networks. *J. Intell. Manuf.* **2020**, *31*, 885–897. [CrossRef]
65. Elias, M.Z.; Malamas, N.; Petrakis Euripides, G.M. A survey on industrial vision systems, applications and tools. *Image Vis. Comput.* **2003**, *2*, 171–188. [CrossRef]
66. Saif, Y.; Yusof, Y.; Latif, K.; Kadir, A.Z.A.; Ahmad, M.B.I.; Adam, A.; Hatem, N. Development of a smart system based on STEP-NC for machine vision inspection with IoT environmental. *Int. J. Adv. Manuf. Technol.* **2021**, *118*, 4055–4072. [CrossRef]